Accepted to the Astrophysical Journal
Preprint typeset using LaTeX style emulateapj v. 04/17/13

SLAC-PUB-153836

# DISCOVERY OF GEV EMISSION FROM THE CIRCINUS GALAXY WITH THE *FERMI*-LAT

Masaaki Hayashida[1,2,3], Łukasz Stawarz[4,5], Chi C. Cheung[6], Keith Bechtol[7], Greg M. Madejski[2], Marco Ajello[8], Francesco Massaro[2], Igor V. Moskalenko[2], Andrew Strong[9], and Luigi Tibaldo[2]

*Accepted to the Astrophysical Journal*

## ABSTRACT

We report the discovery of $\gamma$-ray emission from the Circinus galaxy using the Large Area Telescope (LAT) onboard the *Fermi Gamma-ray Space Telescope*. Circinus is a nearby ($\sim 4$ Mpc) starburst with a heavily obscured Seyfert-type active nucleus, bipolar radio lobes perpendicular to the spiral disk, and kpc-scale jet-like structures. Our analysis of 0.1–100 GeV events collected during 4 years of LAT observations reveals a significant ($\simeq 7.3\,\sigma$) excess above the background. We find no indications of variability or spatial extension beyond the LAT point-spread function. A power-law model used to describe the $0.1-100$ GeV $\gamma$-ray spectrum yields a flux of $(18.8\pm5.8)\times10^{-9}\,\mathrm{ph\,cm^{-2}\,s^{-1}}$ and photon index $2.19\pm0.12$, corresponding to an isotropic $\gamma$-ray luminosity of $3\times10^{40}\,\mathrm{erg\,s^{-1}}$. This observed $\gamma$-ray luminosity exceeds the luminosity expected from cosmic-ray interactions in the interstellar medium and inverse Compton radiation from the radio lobes. Thus the origin of the GeV excess requires further investigation.

*Subject headings:* radiation mechanisms: non-thermal — galaxies: active — galaxies: individual (Circinus) — galaxies: jets — galaxies: Seyfert — gamma rays: galaxies

## 1. INTRODUCTION

Active galactic nuclei (AGN) often possess fast nuclear outflows and collimated radio-emitting jets powered by accretion onto supermassive black holes (e.g., Krolik 1999). Relativistic jets produced in radio-loud AGN (such as blazars and radio galaxies), which are typically hosted by early-type galaxies, are well-established sources of Doppler-boosted $\gamma$-ray emission, dominating the extragalactic source population in the GeV range (Nolan et al. 2012). The bulk of the observed $\gamma$-ray jet emission in such systems is believed to originate within a few parsecs of the central black hole (e.g., Abdo et al. 2010a). However, *Fermi*-LAT observations of nearby radio galaxies indicate that large-scale structures — hereafter 'lobes' or 'bubbles' — formed by jets outside their hosts due to interactions with the intergalactic medium, can also be bright GeV emitters (Abdo et al. 2010b; see also Katsuta et al. 2013).

Radio-quiet AGN, the most luminous of which are classified as Seyferts by their optical spectra, are typically hosted by late-type galaxies. The 'radio-quiet' label does not necessarily mean these sources are completely' radio-silent', and the nuclear jets found in these systems are non-relativistic and comparatively low-powered (e.g., Lal et al. 2011), so that AGN and starburst activities may both be equally important factors in forming of kpc-scale outflows and lobes (e.g., Gallimore et al. 2006). Seyfert galaxies seem $\gamma$-ray quiet as a class (Teng et al. 2011; Ackermann et al. 2012a).

Besides radio-loud AGN, another class of established extragalactic $\gamma$-ray sources consists of galaxies lacking any pronounced nuclear activity, but experiencing a burst of vigorous star formation. The observed GeV emission from these sources is most readily explained by interactions of galactic cosmic rays (CRs) with ambient matter and radiation fields of the interstellar medium (ISM; Ackermann et al. 2012b, and references therein). Starburst-driven outflows routinely found in such systems may lead to the formation of large-scale bipolar structures extending perpendicular to the galactic disks, and somewhat resembling jet-driven AGN lobes (Veilleux et al. 2005).

Circinus is one of the nearest (distance $D = 4.2 \pm 0.7$ Mpc; Tully et al. 2009) and most extensively studied composite starburst/AGN systems, but its location behind the intense foreground of the Milky Way disk, $(l,\, b) = (311.3^\circ,\, -3.8^\circ)$, resulted in exclusion from several previous population studies using LAT data (Ackermann et al. 2012a,b). Circinus exhibits a polarized broad H$\alpha$ line with FWHM $\sim 3000\,\mathrm{km\,s^{-1}}$ (Oliva et al. 1998), evidencing a heavily obscured Seyfert 2 nucleus which ranks as the third brightest Compton-thick AGN (Yang et al. 2009). Radio observations have mapped bipolar bubbles extending orthogonal to the spiral host, as well as kpc-scale jet-like structures likely responsible for the formation of the lobes (Elmouttie et al. 1998). The extended morphology of the system including the lobes has been recently resolved and studied in X-rays (Mingo et al. 2012).

Here, we report the discovery of a significant $\gamma$-ray excess positionally coinciding with the Circinus galaxy

[1] Institute for Cosmic Ray Research, University of Tokyo, 5-1-5 Kashiwanoha, Kashiwa, Chiba, 277-8582, Japan
[2] Kavli Institute for Particle Astrophysics and Cosmology, SLAC National Accelerator Laboratory, Stanford University, 2575 Sand Hill Road M/S 29, Menlo Park, CA 94025, USA
[3] email: mahaya@icrr.u-tokyo.ac.jp
[4] Institute of Space and Astronautical Science, JAXA, 3-1-1 Yoshinodai, Chuo-ku, Sagamihara, Kanagawa 252-5210, Japan
[5] Astronomical Observatory, Jagiellonian University, ul. Orla 171, 30-244 Kraków, Poland
[6] Space Science Division, Naval Research Laboratory, Washington, DC 20375-5352, USA
[7] Kavli Institute for Cosmological Physics, University of Chicago, 5640 South Ellis Avenue, Chicago, IL 60637
[8] Space Sciences Laboratory, 7 Gauss Way, University of California, Berkeley, CA 94720-7450, USA
[9] Max-Planck Institut für extraterrestrische Physik, 85748 Garching, Germany

*Published in arXiv:1310.1913.*

*Work supported in part by US Department of Energy under contract DE-AC02-76SF00515.*

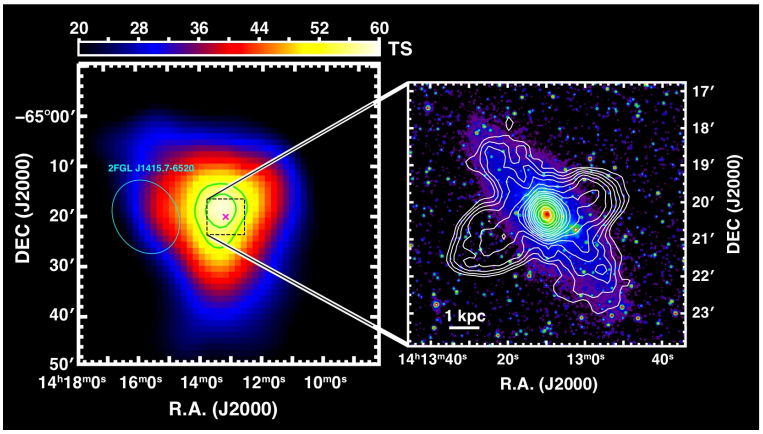


FIG. 1.— The left color map represents the $1^\circ \times 1^\circ$ ($0^\circ.02$ pixels) spatial TS variation of the $> 100$ MeV $\gamma$-ray signal excess centered on Circinus. The green lines denote positional errors of the $\gamma$-ray excess at 68 % and 95 % confidence levels for inner and outer lines, respectively. The magenta cross indicates the position of the galaxy core while the cyan ellipse corresponds to the positional error at 95% confidence of 2FGL J1415.7−6520. The black square corresponds to the area of the right panel, which shows the Australia Telescope Compact Array (ATCA) 1.4 GHz radio contours at $\simeq 20''$ resolution (Elmouttie et al. 1998) superposed with the 2MASS $H$-band color image (Jarrett et al. 2003); here the galactic disk extends in the NE–SW direction, while the radio lobes in the SE–NW direction.

using 4 years of *Fermi*-LAT data and discuss possible origins for this emission.

## 2. LAT DATA ANALYSIS AND RESULTS

The LAT is a pair-production telescope onboard the *Fermi* satellite with large effective area (6500 $\mathrm{cm}^2$ on axis for $> 1$ GeV photons) and large field of view (2.4 sr), sensitive from 20 MeV to $> 300$ GeV (Atwood et al. 2009). Here, we analyzed LAT data for the Circinus region collected between 2008 August 5 and 2012 August 5, following the standard procedure[10], using the LAT analysis software `ScienceTools v9r29v0` with the `P7SOURCE_V6` instrument response functions. Events in the energy range 0.1–100 GeV were extracted within a $17^\circ \times 17^\circ$ region of interest (RoI) centered on the galaxy core position (RA = 213.°2913, Dec = −65.°3390: J2000). $\gamma$-ray fluxes and spectra were determined by a maximum likelihood fit with `gtlike` for events divided into 0.°1-sized pixels and 30 uniformly-spaced log-energy bins. The background model included all known $\gamma$-ray sources within the RoI from the 2nd LAT catalog (2FGL: Nolan et al. 2012), except for 2FGL J1415.7−6520, located 0.°266 away from Circinus. Additionally, the model included the isotropic and Galactic diffuse emission components[11]; flux normalizations for the diffuse and background sources were left free in the fitting procedure.

Our analysis yields a test statistic (TS) of 58 for the maximum likelihood fit when placing a new candidate source at the core position of Circinus, corresponding to a formal detection significance of $\simeq 7.3\,\sigma$. Figure 1 shows the spatial variation in the TS value for the candidate source when evaluated over a grid of positions around the galaxy (TS map). Circinus is located within the 68% confidence region for the direction of the $\gamma$-ray excess. The distribution of the $\gamma$-ray excess is consistent with a point-like feature, but we note that the LAT does not have sufficient angular resolution (see e.g., Ackermann et al. 2013b) to spatially resolve the core, the radio lobes, or the galactic disk (all shown in the right panel of Figure 1)

[10] `http://fermi.gsfc.nasa.gov/ssc/data/analysis/`
[11] `iso_p7v6source.txt` and `gal_2yearp7v6_v0.fits`

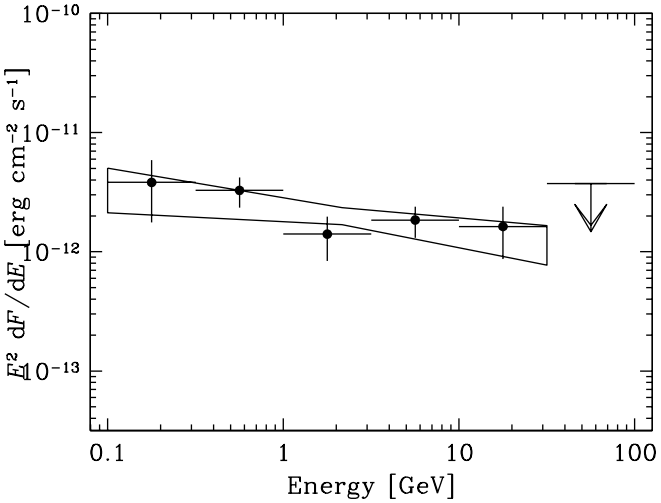


FIG. 2.— GeV spectrum of Circinus as measured by LAT. The black lines represent the best-fit PL model ($1\,\sigma$ confidence band). The vertical bars denote $1\,\sigma$ statistical errors for the flux estimates within energy bins given by horizontal bars. The arrow denotes a 95% confidence level upper limit.

of the system.

Assuming 2FGL J1415.7−6520 is an additional $\gamma$-ray source distinct from the Circinus galaxy, we repeat the analysis including 2FGL J1415.7−6520 in the background model. The $\gamma$-ray excess at the position of Circinus yields in such a case a TS of 52, while no significant excess can be seen at the formal position of 2FGL J1415.7−6520 (TS $\simeq 5.6$). Our analysis confirms therefore a single point-like $\gamma$-ray excess positionally coinciding with Circinus, which may be identified with 2FGL J1415.7−6520 after the localization of the 2FGL source is refined using the 4 year-accumulation of LAT data. The 2FGL analysis flagged 2FGL J1415.7−6520 as a source with a low signal-to-background ratio (2FGL flag was set to '4 '), meaning its position can be relatively strongly affected by systematic uncertainties in the Galactic diffuse emission model (see also Ackermann et al. 2012c), and the overall positional error of

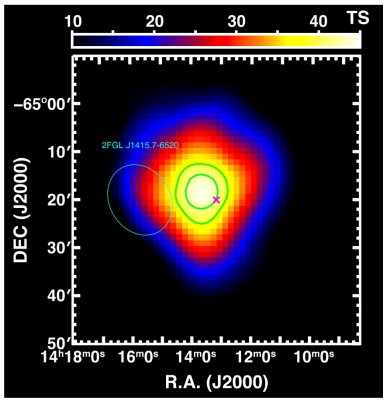


FIG. 3.— The color map represents the $1° \times 1°$ ($0°.02$ pixels) spatial TS variation of the $> 1$ GeV $\gamma$-ray signal excess centered on Circinus. The green lines denote positional errors of the $\gamma$-ray excess at 68 % and 95 % confidence levels. The magenta cross indicates the position of the galaxy core while the cyan ellipse corresponds to the positional error at 95% confidence of 2FGL J1415.7−6520.

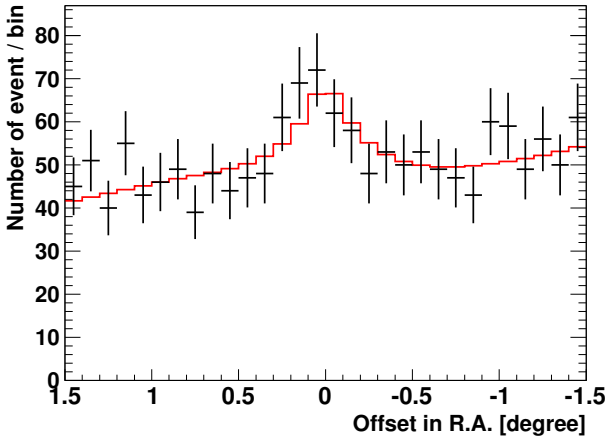


FIG. 4.— Observed counts profile of $> 1$ GeV $\gamma$ rays for the Circinus source with events within $\pm 0.5$ degree in Declination (north-south) projected along the R.A. (east-west) direction. The x-axis represent the offset from the core position of Circinus in R.A. The red curve represents the best-fit emission model with the point-like source and diffuse emission. The observed profile is consistent with a point-like source, indicating no significant spatial extension in the $\gamma$-ray excess associated with Circinus.

2FGL J1415.7−6520 could be larger than indicated. Our analysis here of 4 years of accumulated LAT data for the source allowed it to be detected at higher energies, thus decreasing the systematic uncertainty in the location.

A simple power-law model (PL) adequately describes the $\gamma$-ray spectrum of the source, yielding a $\gamma$-ray flux $\mathcal{F}_{>0.1\,\mathrm{GeV}} = (18.8 \pm 5.8) \times 10^{-9}\,\mathrm{ph\,cm^{-2}\,s^{-1}}$ and photon index $\Gamma = 2.19 \pm 0.12$, corresponding to an isotropic 0.1−100 GeV luminosity of $L_\gamma \simeq (2.9 \pm 0.5) \times 10^{40}\,\mathrm{erg\,s^{-1}}$. The best-fit model together with flux points of the spectral energy distribution (SED) are plotted in Figure 2. We also perform spectral fits using a broken power-law model and a log-parabola model, but no significant improvement ($< 1.2\,\sigma$) can be seen in the likelihood values when compared with the PL parametrization. The results of the spectral fits for Circinus are summarized in Table 1. For comparison, we also derived $\gamma$-ray fluxes and

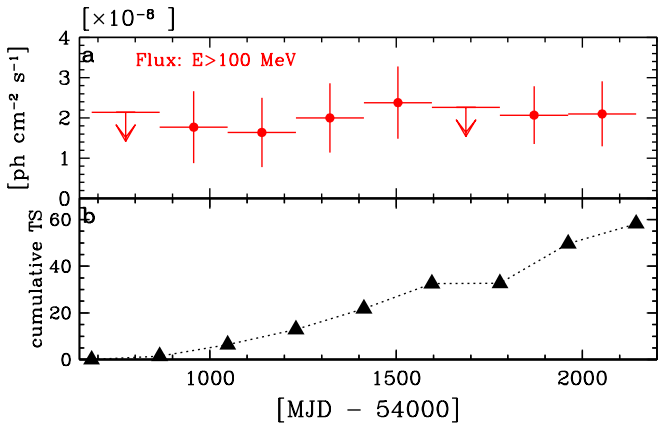


FIG. 5.— The top panel (a) shows the light curve of Circinus above 100 MeV, binned in half-year intervals. For bins with TS $< 4$, a 95 % confidence level upper limit is plotted. The bottom panel (b) presents the cumulative TS of the $\gamma$-ray excess at the source position.

spectra for four LAT-detected starburst galaxies (Ackermann et al. 2012b) with 4-yr LAT data by performing the same analysis procedure described above, and summarize the results in Table 1.

Since Circinus is located near the Galactic plane, it is important to consider systematic errors caused by uncertainties in the Galactic diffuse emission model. We test eight alternative diffuse models (following Ackermann et al. 2013a; de Palma et al. 2013), and find that the derived source flux above 0.1 GeV shifts by no more than 3%, which is much smaller than the statistical uncertainty. The detection significance at the source position remains stable for the different alternative diffuse models (TS $\simeq 58 - 60$).

We also analyze a limited event sample with an energy range $1 - 100$ GeV within a $10° \times 10°$ RoI. In this energy range, reduced systematic effects related to diffuse emission modeling are expected, owing in part to the improved spatial resolution of the LAT. The power-law character of the $\gamma$-ray continuum is confirmed with $\Gamma = 2.19 \pm 0.41$, and we find that much of the statistical power of our search comes from photons above 1 GeV (TS = 42). The extrapolated flux above 0.1 GeV from the higher energy analysis corresponds to $(16.4 \pm 5.6) \times 10^{-9}\,\mathrm{ph\,cm^{-2}\,s^{-1}}$, in good agreement with the result obtained using events from 0.1 GeV. Figure 3 shows a TS map created using events with this energy band, and we have confirmed that Circinus is located at the edge of the 68% confidence contour of the $\gamma$-ray source. We also produced an observed counts profile of Circinus and compared it with the best-fit point-like source model as shown in Figure 4. The observed counts profile is consistent with the model shape of a point-like source, indicating no significant spatial extension of the $\gamma$-ray excess.

In order to search for variability in the $\gamma$-ray flux, we divided the 4-year observation window into half-year intervals and derived $\gamma$-ray fluxes above 0.1 GeV for each time interval using a PL model with photon index fixed at the best-fit value obtained for the 4-year dataset. No significant variability is found in the $\gamma$-ray flux ($\chi^2$/d.o.f = 5.2/7). We also checked the cumulative significance of the $\gamma$-ray excess at the source position

TABLE 1
STARBURST GALAXIES DETECTED WITH *Fermi*-LAT.

| Name | $D$ Mpc | $L_{\rm IR}/10^{44}$ erg s$^{-1}$ | $L_{\rm R}/10^{38}$ erg s$^{-1}$ | TS | $\mathcal{F}_{>0.1\,\rm GeV}$ $10^{-9}$ ph cm$^{-2}$ s$^{-1}$ | $\Gamma$ | $L_\gamma/10^{40}$ erg s$^{-1}$ | $L_\gamma/L_{\rm IR}$ $\times10^{-4}$ | $L_\gamma/L_{\rm R}$ $\times10^{-2}$ |
|---|---|---|---|---|---|---|---|---|---|
| Circinus | 4.2 | 0.60 | 0.45 | 58 | $18.8 \pm 5.8$ | $2.19 \pm 0.12$ | $2.9 \pm 0.5$ | $4.9 \pm 0.9$ | $6.6 \pm 1.1$ |
| NGC 253 | 2.5 | 0.69 | 0.59 | 135 | $10.7 \pm 2.1$ | $2.18 \pm 0.09$ | $0.60 \pm 0.07$ | $0.87 \pm 0.10$ | $1.02 \pm 0.12$ |
| M 82 | 3.4 | 2.0 | 1.5 | 205 | $16.2 \pm 2.3$ | $2.25 \pm 0.08$ | $1.47 \pm 0.14$ | $0.74 \pm 0.07$ | $0.99 \pm 0.09$ |
| NGC 4945 | 3.7 | 1.0 | 1.5 | 42 | $7.2 \pm 2.4$ | $2.05 \pm 0.13$ | $1.17 \pm 0.23$ | $1.13 \pm 0.22$ | $0.77 \pm 0.15$ |
| NGC 1068 | 16.7 | 11 | 23 | 46 | $7.3 \pm 2.9$ | $2.29 \pm 0.19$ | $15.0 \pm 2.9$ | $1.41 \pm 0.27$ | $0.64 \pm 0.12$ |

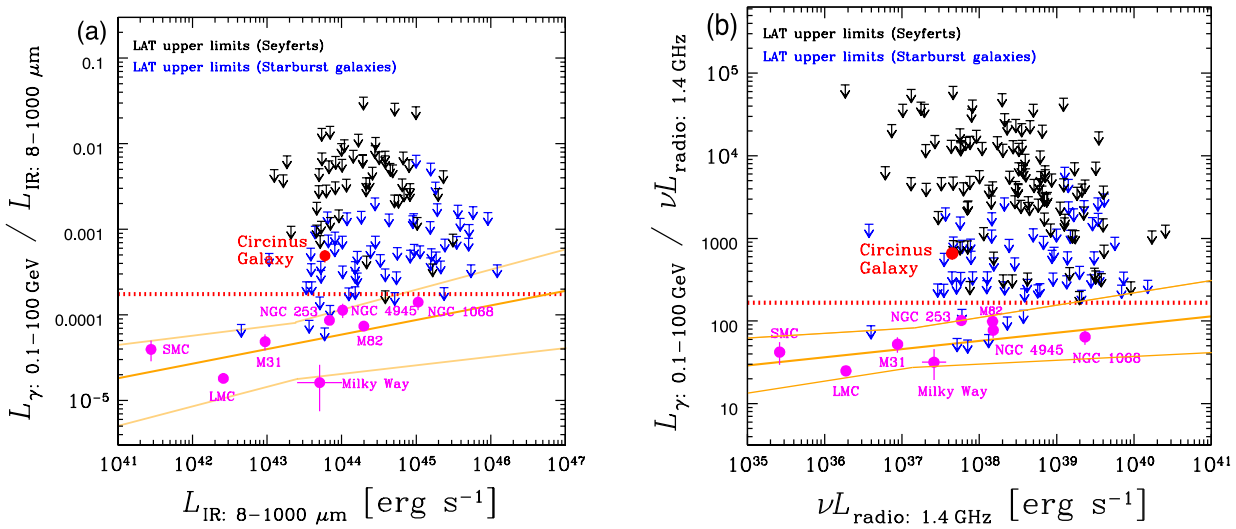


FIG. 6.— Comparisons between (a:left) the $\gamma$-ray (0.1-100 GeV) and total IR ($8-1000\,\mu$m), (b:right) the $\gamma$-ray and 1.4 GHz radio luminosities of star-forming galaxies and Seyferts. Circinus is denoted by the red filled circle. Eight $\gamma$-ray detected star-forming galaxies are plotted by magenta points. $\gamma$-ray upper limits for non-detected starburst galaxies selected from the HCN survey are denoted by blue arrows, and for hard X-ray selected Seyfert galaxies by black arrows. The orange line represents the best-fit power-law relation between $L_\gamma$ and $L_{\rm IR}$ (or $\nu L_{\rm radio}$) for star-forming galaxies, and the orange bands includes the fit uncertainty and intrinsic dispersion around the fitted relation. The dotted red line corresponds to the calorimetric limit assuming an average CR luminosity per supernova of $\eta E_{\rm SN} = 10^{50}$ erg.

during the 4-year observation; the TS showed a gradual increase, as expected for a steady source. Both the source light curve and the cumulative TS are presented in Figure 5.

## 3. DISCUSSION

In Figure 6, we plot the $\gamma$-ray luminosity of Circinus, $L_\gamma$, normalized by the total IR ($8-1000\,\mu$m) luminosity, $L_{\rm IR}$, as a function of $L_{\rm IR}$. For comparison, the plot includes $\gamma$-ray upper limits (95% confidence level) derived for a large sample of starbursts selected from the HCN survey, together with eight $\gamma$-ray detected star-forming galaxies (the four Local Group galaxies and four starbursts). These all follow Ackermann et al. (2012b), with the exception of the four starbursts where the results are from our updated 4-yr LAT analysis (Table 1). In addition, we also show the $\gamma$-ray upper limits for the sample of hard X-ray selected Seyferts (Ackermann et al. 2012a). The IR luminosities are derived from the fluxes measured by the Infrared Astronomical Satellite (IRAS) in four bands, following Sanders & Mirabel (1996).

As shown in Figure 6, and discussed quantitatively in Ackermann et al. (2012b), the $\gamma$-ray emission related to CRs in the ISM scales with the total IR luminosity, which serves as a proxy for the injected CR power within the supernova remnant paradigm for galactic CR origin. Circinus is more than five times over-luminous in the $\gamma$-ray band when compared with this scaling relation (see also Table 1). In fact, the $L_\gamma/L_{\rm IR}$ luminosity ratio for Circinus exceeds the so-called 'calorimetric limit' expected to hold when CRs interact faster than they can escape the galactic disk, and as much as $\eta \simeq 10\,\%$ energy per supernova explosion goes into CR acceleration, $\eta E_{\rm SN} \simeq 10^{50}$ erg (see, e.g., Lacki et al. 2011; Ackermann et al. 2012b). Circinus also does not follow the correlation found for star-forming galaxies between $L_\gamma$ and total monochromatic 1.4 GHz radio luminosity $\nu L_{\rm R}$, by a factor of six (see Table 1 and the right panel of Figure 6). Following the approach of Ackermann et al. (2012b), and assuming that star-forming galaxies do follow a simple power-law scaling between $\gamma$-ray and total-IR luminosity, we find that adjusting either the normalization of this relation or the intrinsic scatter to accommodate Circinus would tend to overpredict the total number of galaxies which have been actually detected by LAT.

Let us consider the possibility that the total IR and radio luminosities listed in Table 1 underestimate the star formation rate (SFR). Whereas standard scaling relations using IRAS fluxes yield SFR $\simeq 2\,{\rm M}_\odot\,{\rm yr}^{-1}$, the most recent mid-IR studies of Circinus with *Spitzer* presented by For et al. (2012) suggest SFR $\simeq (3-8)\,{\rm M}_\odot\,{\rm yr}^{-1}$

(depending on the particular calibration method). The differences between SFRs derived from mid-IR and total-IR (IRAS) measurements might be explained if Circinus is a relatively dust-poor system for which the far-IR luminosity is not a reliable indicator of the SFR. The SFR converted from the observed total 1.4 GHz fluxes (Yun et al. 2001) is only $\simeq 1.5\,M_\odot\,\mathrm{yr}^{-1}$, but the radio luminosity could also under-represent the actual CR injection power if the interstellar magnetic field strength were below average. On the other hand, the total flux density ratio $\log(F_{70\,\mu\mathrm{m}}/F_{1.4\,\mathrm{GHz}}) = 2.40$ demonstrates that Circinus obeys the 'far-IR/radio' correlation established for local star-forming and starburst systems (e.g., Seymour et al. 2009). The luminosities of NGC 1068 and NGC 4945, which are similar starburst/Seyfert composite galaxies, are consistent with the $\gamma$-ray-to-total-IR and $\gamma$-ray-to-radio correlations (Ackermann et al. 2012b, see also Figure 6). These complexities in the Circinus system make a firm conclusion regarding the attribution of $\gamma$ rays to CR interactions difficult.

Other than CR interactions, the disk coronae or accretion disks of Seyfert galaxies can be considered as possible $\gamma$-ray emission sites (e.g., Niedźwiecki et al. 2013). However, LAT studies of a large sample of hard X-ray–selected Seyferts devoid of prominent jets revealed that such sources are $\gamma$-ray quiet as a class, down to the level of $1-10\%$ of the hard X-ray fluxes (Ackermann et al. 2012a).

One of the striking characteristics of the Circinus system is the presence of well-defined radio lobes and kpc-scale jet-like features, the 'plumes' (Elmouttie et al. 1998), which are also resolved at X-ray frequencies with *Chandra* (Mingo et al. 2012). Both of these might be relevant $\gamma$-ray emission sites. To investigate this idea quantitatively, we apply standard leptonic synchrotron and inverse-Compton (IC) modeling to the radio spectra of the lobes, investigating whether the extrapolation of the high-energy emission continuum may account for the GeV flux from the system. In the IC calculations we consider seed photons provided by the cosmic background radiation, the observed IR–to–optical emission of the galactic disk, as well as the UV–to–hard X-ray photon field due to the active nucleus, corrected for obscuration (assuming the intrinsic UV emission of the accretion disk $\simeq 3\times10^{43}\,\mathrm{erg\,s}^{-1}$; Prieto et al. 2010).

Figure 7 presents the broad-band, multi-component SED of Circinus, including new LAT measurements. Integrated far-IR–to–optical measurements represent the dominant starlight and the dust emission of the galaxy, with a negligible contribution from a heavily obscured AGN. In the X-ray regime, the hard X-ray fluxes are dominated by the heavily absorbed emission of the accretion disk and disk coronae. As demonstrated in Elmouttie et al. (1998), the total radio fluxes of the source in the $0.4-8.6$ GHz range are due to a superposition of various emission components characterized by different spectral properties. Using their published ATCA 1.4, 2.4, 4.8, and 8.6 GHz maps, we measured fluxes for each distinct component separately, namely for the nucleus (circle with radius, $r = 1'' \simeq 20$ pc), galaxy core including the central starburst region ($r = 35''$ circle), the outer parts of the galaxy disk, NW lobe ($r = 44.6''$ circle), NW plume ($50''\times25''$ box centered $68.15''$ from the nucleus), SE lobe (ellipse with radii of $70''$ and $55''$), and SE plume ($62.5''\times25''$ box centered $89.30''$ from the nucleus). The total radio emission of the Circinus system at $>$ GHz frequencies is dominated by the central starburst region, and at lower frequencies by the outer parts of the galaxy disk; lobes and plumes contribute to the observed emission at the level of 10%; radio emission of the unresolved nucleus is negligible.

We fit the radio spectra of the lobes and plumes, assuming energy equipartition between the radiating electrons and the magnetic field (energy density ratio $u_e/u_B \equiv 1$), and a standard form of the electron energy distribution consisting of a power-law $dN_e/d\gamma \propto \gamma^{-2}$ between electron energies $\gamma_{\mathrm{min}} \equiv 1$ and $\gamma_{\mathrm{br}}$, breaking to $dN_e/d\gamma \propto \gamma^{-3}$ between $\gamma_{\mathrm{br}}$ and $\gamma_{\mathrm{max}} \equiv 10^6$. We adjust both the electron normalization and break Lorentz factors $\gamma_{\mathrm{br}}$ to obtain satisfactory fits to the radio data for each region separately, and then evaluate the expected IC emission. The results of the modeling are given as blue curves in Figure 7, where we show in addition the modeled emission of the accretion disk and the disk coronae using the `MyTORUS` model (red curves) (Murphy & Yaqoob 2009). For comparison, the figure presents also the interstellar radiation field/`GALPROP` models (Porter et al. 2008; Strong et al. 2010) for the Milky Way placed at the distance of Circinus (gray curves). Note that the "clump" structure seen around $10^{23}$ Hz in the $\gamma$-ray continuum evaluated with `GALPROP` is due to the pion decay component dominating over the leptonic (IC and bremsstrahlung) ISM emission.

The evaluated IC emission of the lobes severely underestimates the measured GeV emission of Circinus. In the model, magnetic field intensities read as $B \simeq 5-10\,\mu$G, in agreement with the values claimed by Elmouttie et al. (1998). The total energy stored in the entire structure is $E_{\mathrm{tot}} \simeq 10^{54}$ erg. This is about an order of magnitude lower than the total energy of the lobes inferred by Mingo et al. (2012) based on X-ray observations, indicating either a significant departure from the energy equipartition condition or dominant pressure support within the lobes provided by hot thermal plasma or relativistic protons. The departures from the minimum energy condition $u_e/u_B \gg 1$, which may enhance the expected IC radiation for a given synchrotron (radio) flux, are often claimed for lobes in radio galaxies and quasars (see Takeuchi et al. 2012, and references therein). In the particular case of Circinus, however, the effect would have to be extreme in order to account for the flux detected with the LAT, $u_e/u_B \simeq 10^4$. Although we cannot exclude this possibility, we consider it rather unlikely. Deep, high-resolution X-ray observations could in principle be used in the near future to validate the $u_e/u_B \gg 1$ hypothesis for the Circinus lobes, but at this moment the very limited photon statistics of the available *Chandra* maps precludes any robust detection of a non-thermal lobe-related emission component at keV photon energies. We note however that the IC model curve calculated for $u_e/u_B = 1$ and shown in Figure 7 is below the corresponding upper limits.

Yet another possibility is the presence of an energetically significant population of CR protons associated with the radio lobes. Relativistic protons injected by the kpc-scale jets/plumes, or accelerated at the bow-shocks

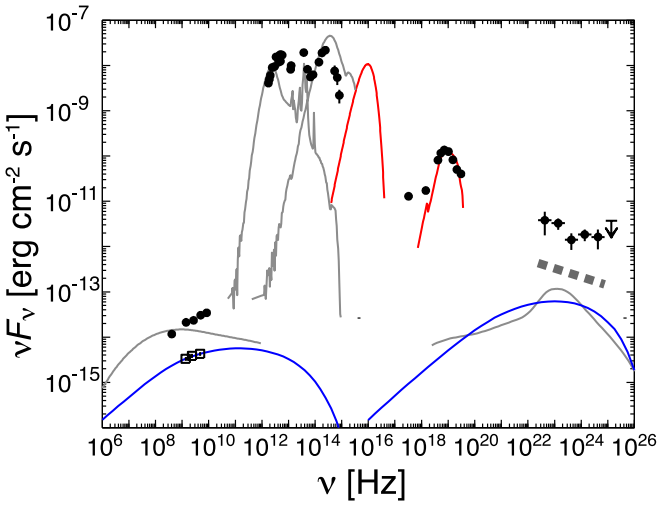


FIG. 7.— Broad-band, multi-component SED of Circinus. Black open squares represent the total 'lobes + plumes' radio fluxes, with the assumed 10% uncertainties. Black filled circles denote the total (integrated) fluxes of the system from the Parkes Catalog ($0.4-8.6$ GHz; Wright & Otrupcek 1990), ISO ($170-52\,\mu$m; Brauher et al. 2008), IRAS ($100-25\,\mu$m), *Spitzer* and 2MASS ($70-1\,\mu$m; For et al. 2012), RC3.9 catalog (extinction-corrected $V$, $B$, and $U$-bands; de Vaucouleurs et al. 1991), ROSAT ($0.1-2.4$ keV; Brinkmann et al. 1994), *Suzaku* ($2-10$ keV; Yang et al. 2009), *Swift*-BAT ($14-195$ keV; Baumgartner et al. 2010) and LAT ($0.1-100$ GeV; this paper). Gray curves correspond to the interstellar radiation field/`GALPROP` models for the Milky Way (Porter et al. 2008; Strong et al. 2010) placed at the distance of Circinus. Red curves denote the modeled emission of the accretion disk and the disk coronae using the `MyTORUS` model. Blue curves represent the modeled synchrotron and IC emission of the lobes and plumes. The thick gray dotted line represents the $\gamma$-ray spectrum of a starforming system (assumed $\Gamma = 2.2$) corresponding to the IR luminosity of Circinus and IR-$\gamma$ correlation found in Ackermann et al. (2012b).

of the expanding lobes (see Mingo et al. 2012), may generate a non-negligible $\gamma$-ray emission due to the decay of pions produced during CR interactions with surrounding matter. However, due to the sparseness of thermal gas within the galactic halo (gas number density $\lesssim 10^{-3}$ cm$^{-3}$), implying a low efficiency for this process, the resulting GeV fluxes are likely below the $\gamma$-ray output of the galactic disk.

It is interesting to comment in this context on the similarities between the Circinus lobes and the *Fermi*-LAT discovered giant 'Fermi Bubbles' in our Galaxy (Dobler et al. 2010; Su et al. 2010). Even though the origin of both structures is still under the debate, the jet activity of their central supermassive black holes — which are of comparable masses, namely $\mathcal{M}_{\rm BH} \simeq (1.7 \pm 0.3) \times 10^6\,M_\odot$ for Circinus (Greenhill et al. 2003) and $(4.5 \pm 0.4) \times 10^6\,M_\odot$ for the Milky Way (e.g., Ghez et al. 2008) — is the widely considered scenario. In the case of Circinus, the jet scenario is evidenced directly by the presence of collimated outflows supplying the lobes with energetic magnetized plasma (see the discussion in Elmouttie et al. 1998; Mingo et al. 2012), while in the case of our Galaxy, it is supported by general energetic arguments and numerical simulations reproducing well the observed properties of bubbles (e.g., Guo & Mathews 2012; Yang et al. 2012). In both systems, the lobes extend to kpc scales across the galactic disks and are characterized by magnetic field strengths of the order of $\sim 10\,\mu$G (see Su et al. 2010; Mertsch & Sarkar 2011, for Fermi Bubbles). Thus it seems that structures analogous to the Fermi Bubbles and Circinus lobes may not be uncommon in late-type galaxies undergoing episodic outbursts of AGN (jet) activity, but their contributions to the total $\gamma$-ray outputs of the systems do not exceed $\sim 10\%$.

## 4. CONCLUSIONS

Here we report the detection of a steady and spatially unresolved $\gamma$-ray source at the position of Circinus, consistent with 2FGL J1415.7−6520 based on a refined analysis using 4 years of LAT data. Although the observed power-law spectrum ($\Gamma = 2.19 \pm 0.12$) is similar to that of other LAT-detected starburst systems, Circinus is $\gamma$-ray over-luminous by a factor of 5–6 relative to what is expected for emission from the ISM, based on multi-wavelength correlations observed for nearby star-forming galaxies. However, the range of SFRs estimated from radio, mid-IR, and far-IR luminosities span a factor of $\simeq 4$, indicating large uncertainties in the expected CR power delivered to the ISM. We presented several alternative possibilities for the origin of the GeV excess, including emission from the extended radio lobes, but found no conclusive answer to fully account for the GeV emission. This issue may be resolved by future studies, as Circinus is a compelling target for observations in the very high energy $\gamma$-ray regime with ground-based Cherenkov telescopes; the TeV-detected starburst systems NGC 253 and M82 (Acero et al. 2009; Acciari et al. 2009) are actually fainter in the GeV range.

## ACKNOWLEDGMENTS

Ł. S. was supported by Polish NSC grant DEC-2012/04/A/ST9/00083. Work by C.C.C. at NRL is supported in part by NASA DPR S-15633-Y.

The *Fermi* LAT Collaboration acknowledges generous ongoing support from a number of agencies and institutes that have supported both the development and the operation of the LAT as well as scientific data analysis. These include the National Aeronautics and Space Administration and the Department of Energy in the United States, the Commissariat à l'Energie Atomique and the Centre National de la Recherche Scientifique / Institut National de Physique Nucléaire et de Physique des Particules in France, the Agenzia Spaziale Italiana and the Istituto Nazionale di Fisica Nucleare in Italy, the Ministry of Education, Culture, Sports, Science and Technology (MEXT), High Energy Accelerator Research Organization (KEK) and Japan Aerospace Exploration Agency (JAXA) in Japan, and the K. A. Wallenberg Foundation, the Swedish Research Council and the Swedish National Space Board in Sweden.

Additional support for science analysis during the operations phase is gratefully acknowledged from the Istituto Nazionale di Astrofisica in Italy and the Centre National d'Études Spatiales in France.

We thank M. Elmouttie for providing the ATCA images.

REFERENCES


Abdo, A. A., Ackermann, M., Ajello, M., et al. 2010a, Nature, 463, 919
Abdo, A. A., Ackermann, M., Ajello, M., et al. 2010b, Science, 328, 725
Acciari, V. A., Aliu, E., et al. 2009, Nature, 462, 770
Acero, F., Aharonian, F., Akhperjanian, A. G., et al. 2009, Science, 326, 1080
Ackermann, M., Ajello, M., Allafort, A., et al. 2012a, ApJ, 747, 104
Ackermann, M., Ajello, M., Allafort, A., et al. 2012b, ApJ, 755, 164
Ackermann, M., Ajello, M., Atwood, W. B., et al. 2012c, ApJ, 750, 3
Ackermann, M., Ajello, M., Allafort, A., et al. 2013a, Science, 339, 807
Ackermann, M., Ajello, M., Allafort, A., et al. 2013b, ApJ, 765, 54
Atwood, W. B., Abdo, A. A., Ackermann, M., et al. 2009, ApJ, 697, 1071
Baumgartner, W. H., Tueller, J., Markwardt, C., & Skinner, G. 2010, Bulletin of the American Astronomical Society, 42, 675
Brauher, J. R., Dale, D. A., & Helou, G. 2008, ApJS, 178, 280
Brinkmann, W., Siebert, J., & Boller, T. 1994, A&A, 281, 355
de Palma, F., Brandt, T. J., Johannesson, G., & Tibaldo, L., for the *Fermi*-LAT collaboration 2013, arXiv:1304.1395
de Vaucouleurs, G., de Vaucouleurs, A., Corwin, H. G., Jr., et al. 1991, Third Reference Catalogue of Bright Galaxies (1991)
Dobler, G., Finkbeiner, D. P., Cholis, I., Slatyer, T., & Weiner, N. 2010, ApJ, 717, 825
Elmouttie, M., Haynes, R. F., Jones, K. L., Sadler, E. M., & Ehle, M. 1998, MNRAS, 297, 1202
For, B.-Q., Koribalski, B. S., & Jarrett, T. H. 2012, MNRAS, 425, 1934
Gallimore, J. F., Axon, D. J., O'Dea, C. P., Baum, S. A., & Pedlar, A. 2006, AJ, 132, 546
Guo, F., & Mathews, W. G. 2012, ApJ, 756, 181
Ghez, A. M., Salim, S., Weinberg, N. N., et al. 2008, ApJ, 689, 1044
Greenhill, L. J., Booth, R. S., Ellingsen, S. P., et al. 2003, ApJ, 590, 162
Jarrett, T. H., Chester, T., Cutri, R., Schneider, S. E., & Huchra, J. P. 2003, AJ, 125, 525
Katsuta, J., Tanaka, Y. T., Stawarz, Ł., et al. 2013, A&A, 550, A66
Krolik, J. H. 1999, Active galactic nuclei: from the central black hole to the galactic environment (Princeton: Princeton University Press)
Lacki, B. C., Thompson, T. A., Quataert, E., Loeb, A., & Waxman, E. 2011, ApJ, 734, 107
Lal, D. V., Shastri, P., & Gabuzda, D. C. 2011, ApJ, 731, 68
Mertsch, P., & Sarkar, S. 2011, Physical Review Letters, 107, 091101
Mingo, B., Hardcastle, M. J., Croston, J. H., et al. 2012, ApJ, 758, 95
Murphy, K. D., & Yaqoob, T. 2009, MNRAS, 397, 1549
Niedźwiecki, A., Xie, F.-G., & Stepnik, A. 2013, MNRAS, 432, 1576
Nolan, P. L., Abdo, A. A., Ackermann, M., et al. 2012, ApJS, 199, 31
Oliva, E., Marconi, A., Cimatti, A., & Alighieri, S. D. S. 1998, A&A, 329, L21
Porter, T. A., Moskalenko, I. V., Strong, A. W., Orlando, E., & Bouchet, L. 2008, ApJ, 682, 400
Prieto, M. A., Reunanen, J., Tristram, K. R. W., et al. 2010, MNRAS, 402, 724
Sanders, D. B., & Mirabel, I. F. 1996, ARA&A, 34, 749
Seymour, N., Huynh, M., Dwelly, T., et al. 2009, MNRAS, 398, 1573
Strong, A. W., Porter, T. A., Digel, S. W., et al. 2010, ApJ, 722, L58
Su, M., Slatyer, T. R., & Finkbeiner, D. P. 2010, ApJ, 724, 1044
Takeuchi, Y., Kataoka, J., Stawarz, Ł., et al. 2012, ApJ, 749, 66
Teng, S. H., Mushotzky, R. F., Sambruna, R. M., Davis, D. S., & Reynolds, C. S. 2011, ApJ, 742, 66
Tully, R. B., Rizzi, L., Shaya, E. J., et al. 2009, AJ, 138, 323
Veilleux, S., Cecil, G., & Bland-Hawthorn, J. 2005, ARA&A, 43, 769
Wright, A., & Otrupcek, R. 1990, PKS Catalog (1990)
Yang, Y., Wilson, A. S., Matt, G., Terashima, Y., & Greenhill, L. J. 2009, ApJ, 691, 131
Yang, H.-Y. K., Ruszkowski, M., Ricker, P. M., Zweibel, E., & Lee, D. 2012, ApJ, 761, 185
Yun, M. S., Reddy, N. A., & Condon, J. J. 2001, ApJ, 554, 803